Stabilization of Trivalent Nickel in Tetragonal NiS_4N_2 and NiN_6 Environments: Synthesis, Structures, Redox Potentials, and Observations Related to [NiFe]-Hydrogenases

H.-J. Krüger and R. H. Holm*

Contribution from the Department of Chemistry, Harvard University, Cambridge, Massachusetts 02138. *Received September 29, 1989*

Abstract: The influence of ligand structure on Ni(III)/Ni(II) redox potentials has been examined in order to elucidate those factors that lead to unusually low values for this couple, such as are found in [NiFe]-hydrogenases. The compound $(Et_4N)_2[Ni(pdtc)_2]$ [**3**, pdtc = pyridine-2,6-bis(monothiocarboxylate)(2-)] is readily prepared and crystallizes in monoclinic space group $C2/c$ with a = 19.036 (4) Å, b = 11.231 (2) Å, c = 16.588 (3) Å, β = 101.01 (1)°, and Z = 4. Reaction of **3** with iodine in methanol and addition of $(Ph_3PCH_2Ph)Br$ affords green $(Ph_3PCH_2Ph)[Ni(pdtc)_2]$ (**4**), which crystallizes in monoclinic space group $P2_1/n$ with a = 10.181 (1) Å, b = 21.033 (4) Å, c = 16.937 (3) Å, β = 95.02 (1)°, and Z = 4. Also prepared was $(Ph_3PCH_2Ph)[Co(pdtc)_2]$, which is isomorphous with **4**. Complexes **3** and **4** and $[Co(pdtc)_2]^{1-}$ have tetragonally distorted octahedral structures in which the tridentate ligand binds in a meridional manner such that each species has an essentially planar MS_4 fragment. The EPR properties of **4** [$g_\perp > g_\parallel$, g_{av} = 2.103, $a_{av}(^{61}Ni)$ = 22 ± 1 G] and comparative structural features with **3** and $[Co(pdtc)_2]^{1-}$ demonstrate the Ni(III) state with a $(d_{z^2})^1$ ground state. Thus, the **3**/**4** redox couple, with $E_{1/2}$ = −0.085 V vs SCE in DMF, is a metal-centered process. $[Ni(pdtc)_2]^{2-,1-}$ are the first pair of structurally defined Ni(II,III) complexes with anionic sulfur ligands. The previously reported Ni(II) complex $[Ni(dapo)_2]^{2-}$ [**5**, dapo = pyridine-2,6-bis(acetyloximate)(2-)] exhibited a three-membered redox series, being oxidized to $[Ni(dapo)_2]^{1-}$ (**6**) and then to the known Ni(IV) complex $[Ni(dapo)_2]$ (**7**) at $E_{1/2}$ = −0.735 and −0.255 V in DMF. The tetragonally distorted octahedral structure established earlier for **7** doubtless applies to **6**, which could not be isolated. However, the EPR spectrum of **6**, although poorly resolved, has g_{av} = 2.086, indicating that the **5**/**6** redox couple is metal-centered. The potential of this couple is one of the two lowest values reported for $Ni^{III/II}$. These results make clear that, in the absence of any pronounced structural stabilization of one oxidation state, the dominant ligand electronic property in lowering redox potentials is the presence of polarizable, electron-rich donor atoms or groups. Low potentials (ca. −400 to −600 mV vs SCE) are a prominent feature of [NiFe]-hydrogenases. Certain properties of these synthetic systems are compared with those of enzymes, and suggestions as to the nature of native Ni sites are offered.

The role of nickel as a trace element in biology is manifested in its occurrence in at least four enzymes of widely different metabolic functions.[1,2] [NiFe]-hydrogenases, enzymes that contain mononuclear nickel sites and Fe–S clusters, are complicated species in which the nickel sites are not well-defined at present.[2,3] One recent example of the complexity and structural variability of these enzymes is the discovery of a [NiFeSe]-hydrogenase, in which a selenocysteinate residue is bound to nickel.[4]

One of the more thoroughly investigated [NiFe]-hydrogenases is that isolated from the sulfate-reducing bacterium *Desulfovibrio gigas*.[3b,5] In the "as prepared" form of the enzyme, the EPR spectrum with g values of 2.31, 2.23, and 2.02 (Ni A spectrum) has been attributed to trivalent nickel in an approximately tetragonal environment. Upon incubation with H_2, this spectrum becomes replaced by a spectrum with g values of 2.19, 2.16, and 2.02 (Ni C spectrum), which corresponds to a Ni(III) intermediate form of the enzyme. At longer incubation times, an EPR-silent state ascribed to Ni(II) is reached. A different interpretation of a similar reaction sequence by another enzyme implicates Ni(I) and Ni(0) states.[6] XANES data for oxidized and fully reduced *D. gigas* hydrogenase do not favor a tetrahedral or planar four-coordinate geometry and rather suggest a pseudooctahedral Ni environment.[7] However, five-coordinate sites could not be ruled out. EXAFS results for the oxidized enzymes from *D. gigas* and *Methanobacterium thermoautotrophicum* have been interpreted in terms of at least three sulfur-containing ligands with Ni–S distances in the range 2.12–2.28 Å.[8] For these same enzymes, electron spin echo spectroscopy indicates the presence of a nitrogen atom, possibly from imidazole, near the Ni atom.[9] If the reduced site is of the NiS_4 type, it is probably not tetrahedral, as in Ni-substituted rubredoxin, inasmuch as recent MCD results for several hydrogenases in reduced conditions indicate the absence of paramagnetic Ni(II).[10]

Probably the most noteworthy characteristics of the Ni sites in [NiFe]-hydrogenases are the existence of stable Ni^{III} states and the low $Ni^{III/II}$ redox potentials, ca. −150 to −400 mV vs NHE.[11]

(1) *The Bioinorganic Chemistry of Nickel*; Lancaster, J. R., Ed.; VCH Publishers, Inc.: New York, 1988.

(2) (a) Hausinger, R. P. *Microbiol. Rev.* **1987**, *51*, 22. (b) Walsh, C. T.; Orme-Johnson, W. H. *Biochemistry* **1987**, *26*, 4901. (c) Cammack, R. *Adv. Inorg. Chem.* **1988**, *32*, 297.

(3) (a) Cammack, R.; Fernandez, V. M.; Schneider, K. In ref. 1, Chapter 8. (b) Moura, J. J. G.; Teixeira, M.; Moura, I.; LeGall, J. In ref. 1, Chapter 9. (c) Bastain, N. R.; Wink, D. A.; Wackett, L. P.; Livingston, D. J.; Jordan, L. M.; Fox, J.; Orme-Johnson, W. H.; Walsh, C. T. In ref. 1, Chapter 10. (d) Moura, J. J. G.; Teixeira, M.; Moura, I. *Pure Appl. Chem.* **1989**, *61*, 915.

(4) (a) Eidsness, M. K.; Scott, R. A.; Prickril, B. C.; DerVartanian, D. V.; LeGall, J.; Moura, I.; Moura, J. J. G.; Peck, H. D., Jr. *Proc. Natl. Acad. Sci. U.S.A.* **1989**, *86*, 147. (b) Shao, H. H.; Teixeira, M.; LeGall, J.; Patil, D. S.; Moura, I.; Moura, J. J. G.; DerVartanian, D. V.; Huynh, B. H.; Peck, H. D., Jr. *J. Biol. Chem.* **1989**, *264*, 2678.

(5) (a) Teixeira, M.; Moura, I.; Xavier, A. V.; Huynh, B. H.; DerVartanian, D. V.; Peck, H. D., Jr.; LeGall, J.; Moura, J. J. G. *J. Biol. Chem.* **1985**, *260*, 8942. (b) Cammack, R.; Patil, D.; Hatchikian, E. C.; Fernandez, V. M. *Biochim. Biophys. Acta* **1987**, *912*, 98. (c) Huynh, B. H.; Patil, D. S.; Moura, I.; Teixeira, M.; Moura, J. J. G.; DerVartanian, D. V.; Czechowski, M. H.; Prickril, B. C.; Peck, H. D., Jr.; LeGall, J. *J. Biol. Chem.* **1987**, *262*, 795. (d) Teixeira, M.; Moura, I.; Xavier, A. V.; Moura, J. J. G.; LeGall, J.; DerVartanian, D. V.; Peck, H. D., Jr.; Huynh, B. H. *J. Biol. Chem.* **1989**, *264*, 16435.

(6) van der Zwaan, J. W.; Albracht, S. P. J.; Fontijn, R. D.; Slater, E. C. *FEBS Lett.* **1985**, *179*, 271.

(7) Eidsness, M. K.; Sullivan, R. J.; Scott, R. A. In ref. 1, Chapter 4.

(8) (a) Lindahl, P. A.; Kojima, N.; Hausinger, R. P.; Fox, J. A.; Teo, B.-K.; Walsh, C. T.; Orme-Johnson, W. H. *J. Am. Chem. Soc.* **1984**, *106*, 3062. (b) Scott, R. A.; Wallin, S. A.; Czechowski, M.; DerVartanian, D. V.; LeGall, J.; Peck, H. D., Jr.; Moura, I. *J. Am. Chem. Soc.* **1984**, *106*, 6864. (c) Scott, R. A.; Czechowski, M.; DerVartanian, D. V.; LeGall, J.; Peck, H. D., Jr.; Moura, I. *Rev. Port. Quim.* **1985**, *27*, 67.

(9) (a) Tan, S.-L.; Fox, J. A.; Kojima, N.; Walsh, C. T.; Orme-Johnson, W. H. *J. Am. Chem. Soc.* **1984**, *106*, 3064. (b) Chapman, A.; Cammack, R.; Hatchikian, E. C.; McCracken, J.; Peisach, J. *FEBS Lett.* **1988**, *242*, 135.

(10) Kowal, A. T.; Zambrano, I. C.; Moura, I.; Moura, J. J. G.; LeGall, J.; Johnson, M. K. *Inorg. Chem.* **1988**, *27*, 1162.

(11) These values correspond to −390 to −640 mV vs SCE. Unless noted otherwise, subsequent potentials refer to the SCE.

0002-7863/90/1512-2955$02.50/0

These values are very much lower than potentials of about +500 mV or higher commonly observed for $Ni^{III/II}$ couples of synthetic compounds.[12] The large majority of complexes with these potentials are neutral or are cations. There are only a limited number of complexes with potentials substantially below this value.[13-16] Among these are tetradentate amidatethiolate species with potentials in the −0.03 to −0.42 V interval.[15] The lowest potential thus far observed is that for bis(norbornane-1,2-dithiolato)Ni(II), which undergoes metal-based oxidation to Ni(III) at $E_{1/2}$ = −0.76 V in DMF.[16] From these examples, one method of lowering $Ni^{III/II}$ potentials is the incorporation of negative, polarizable ligands such as thiolates in complexes of overall negative charge. However, nearly all mononuclear Ni(II) thiolate complexes suffer irreversible, ligand-based oxidation to form disulfides, a property that we addressed in a recent study.[17] Another example of this reaction has just been described.[18] Numerous other Ni(II) thiolates are polynuclear species.[19]

Our premise is that information on the formation, structures, stabilities, and reactions of Ni(III) complexes with *anionic* sulfur ligation could be useful in interpreting similar properties of Ni(III) in hydrogenases. Therefore, we have sought additional routes to stable Ni(III) species with this ligation mode. The approach presented here utilizes the dianion **1** (pdtc) of pyridine-2,6-bis-

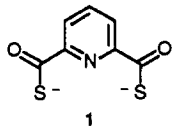

1

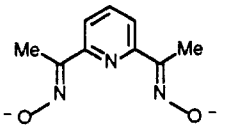

2

(monothiocarboxylic acid), a natural product of some strains of *Pseudomonas putida* when grown under conditions of iron deficiency.[20] The reduced basicities and higher redox potentials of monothio acids (vide infra) are features that, relative to thiolates RS^-, are not expected to favor bridge formation or intramolecular redox reactions. The preparation of the stable Fe(III) complex $[Fe(pdtc)_2]^{1-}$[21a] is consistent with these expectations.

Among other polarizable anionic ligands known to stabilize high oxidation states of nickel are deprotonated oximes,[12,22-24] among them dianion **2** (dapo) of pyridine-2,6-bis(acetyloxime). This ligand has been reported to form six-coordinate Ni(II) and Ni(IV) complexes, but not an intermediate Ni(III) species.[22] Here we present an investigation of the nickel complexes of **1** and **2**, the results of which are considered in relation to the general problem of stabilizing Ni(III) and to the nature of the nickel sites in hydrogenases.

Table I. Crystallographic Parameters for $(Et_4N)_2[Ni(pdtc)_2]$ (A), $(Ph_3PCH_2Ph)[Ni(pdtc)_2]$ (B), and $(Ph_3PCH_2Ph)[Co(pdtc)_2]$ (C)

	A	B	C
chem formula	$C_{30}H_{46}N_4NiO_4S_4$	$C_{39}H_{28}N_2NiO_4PS_4$	$C_{39}H_{28}N_2CoO_4PS_4$
mw	713.69	806.61	806.83
a, Å	19.036 (4)	10.181 (1)	10.112 (1)
b, Å	11.231 (2)	21.033 (4)	21.152 (4)
c, Å	16.588 (3)	16.937 (3)	16.911 (2)
β, deg	101.01 (1)	95.02 (1)	94.96 (1)
V, Å^3	3481 (1)	3613 (1)	3603 (1)
Z	4	4	4
space group	$C2/c$ (No. 15)	$P2_1/n$ (No. 14)	$P2_1/n$ (No. 14)
T, K	298	298	298
λ, Å	0.71069	0.71069	0.71069
d_{calc} (d_{obsd}), g/cm^3	1.36 (1.36)[a]	1.48 (1.48)[a]	1.49 (1.49)[a]
μ, cm^{-1}	8.27	8.47	7.84
$R(F_o)$	3.12	3.85	3.89
$R_w(F_o^2)$	3.97	4.00	3.89

[a] Determined by neutral buoyancy in CCl_4–hexanes.

Experimental Section

Preparation of Compounds. Pyridinium pyridinium-2,6-bis(monothiocarboxylate) ((pyH)(pdtcH)) was prepared by the slow addition of pyridine-2,6-bis(carbonyl chloride) to a saturated H_2S solution in pyridine.[25] The complexes $Na_2[Ni(dapo)_2]$ and $Ni(dapo)_2$ were obtained by the methods of Baucom and Drago.[22]

$(Et_4N)_2[Ni(pdtc)_2]$. In 75 mL of boiling ethanol containing 3.2 g of a 25% methanolic Et_4NOH solution was dissolved 0.900 g (3.24 mmol) of (pyH)(pdtcH). To this solution was added 0.373 g (1.50 mmol) of $Ni(OAc)_2 \cdot 4H_2O$ as a solid. The brown solution was maintained at the boiling temperature until all of the red material at the bottom of the flask disappeared and only brown crystals were visible (ca. 10 min). The solution was cooled to room temperature and then to −30 °C, where it was maintained for 1 h. The brown crystalline precipitate was collected by filtration, washed with 10–20 mL of cold ethanol and with ether to afford 0.984–1.010 g (92–94%) of product. An analytical sample was obtained by recrystallization from hot ethanol as large dark-brown needles. Anal. Calcd for $C_{30}H_{46}N_4NiO_4S_4$: C, 50.49; H, 6.50; N, 7.85; Ni, 8.23; S, 17.97. Found: C, 50.45; H, 6.42; N, 7.89; Ni, 8.28; S, 18.40. ^1H NMR (Me_2SO-d_6, anion): δ 20.0 (1), 65.8 (2). Absorption spectrum (DMF): λ_{max} (ϵ_M) 342 nm (16 200), 548 (sh, 197), 859 (83.5), 1050 (sh, 32.0). IR (KBr): 1553, 1536, 1478, 1471, 1451, 1245, 1184, 946, 833, 752, 674 cm^{-1} (strong bands only).

$(Et_4N)[Ni(pdtc)_2]$. Under a dinitrogen atmosphere, a solution of 0.153 g (0.603 mmol) of iodine in 30 mL of methanol was added dropwise over 15 min to a filtered solution of 0.984 g (1.38 mmol) of $(Et_4N)_2[Ni(pdtc)_2]$ in 80 mL of methanol. The color of the reaction mixture immediately became greenish and a fine crystalline precipitate appeared during the addition. The mixture was filtered, and the product was washed thoroughly with 5 × (10–20) mL of methanol and twice with ether. After being dried in vacuo, the product was obtained as 0.598 g (85%) of dark green microcrystalline solid. Anal. Calcd for $C_{22}H_{26}N_3NiO_4S_4$: C, 45.29; H, 4.49; N, 7.20; Ni, 10.06; S, 21.98. Found: C, 45.12; H, 4.42; N, 7.84; Ni, 10.06; S, 22.26. Absorption spectrum (DMF): λ_{max} (ϵ_M) 308 nm (11 300), 353 (19 200), 380 (sh, 15 800), 610 (3820), 782 (sh, 424), 1270 (313). IR (KBr): 1607, 1577, 1489, 1246, 1173, 911, 823, 746, 668 cm^{-1} (strong bands only).

To obtain a compound suitable for X-ray structural analysis, the preceding compound was dissolved in acetone–water and the anion was precipitated by addition of an aqueous solution of $(Ph_3PCH_2Ph)Br$. This material was collected and dried in vacuo.

$(Et_4N)[Co(pdtc)_2]$. A solution of 0.373 g (1.50 mmol) of $Co(OAc)_2 \cdot 4H_2O$ in 8 mL of methanol was added to a solution prepared from 0.900 g (3.24 mmol) of (pyH)(pdtcH), 0.380 g (6.77 mmol) of KOH, and 0.248 g (1.50 mmol) of Et_4NCl in 50 mL of hot methanol. The crystalline product that separated from the brown solution was collected by filtration, washed with 2 × 20 mL of water, 20 mL of methanol, and ether, to afford 0.809 g (92%) of product. An analytical sample was prepared by recrystallization from hot acetonitrile as flaky orange-brown crystals. Anal. Calcd for $C_{22}H_{26}CoN_3O_4S_4$: C, 45.27; H, 4.49; N, 7.20; S, 21.97. Found: C, 45.43; H, 4.48; N, 7.27; S, 21.70. ^1H NMR (Me_2SO-d_6, anion): δ 7.95 (d, 2), 8.34 (t, 1). Absorption spectrum

(12) (a) Nag, K.; Chakravorty, A. *Coord. Chem. Rev.* **1980**, *33*, 87. (b) Haines, R. J.; McAuley, A. *Coord. Chem. Rev.* **1981**, *39*, 77. (c) Lappin, A. G.; McAuley, A. *Adv. Inorg. Chem.* **1988**, *32*, 241.
(13) Busch, D. H. *Acc. Chem. Res.* **1978**, *11*, 392.
(14) Chakravorty, A. *Isr. J. Chem.* **1985**, *25*, 99.
(15) Krüger, H.-J.; Holm, R. H. *Inorg. Chem.* **1987**, *26*, 3645, and unpublished results.
(16) Fox, S.; Silver, A.; Wang, Y.; Millar, M. Abstracts of the Fourth International Conference on Bioinorganic Chemistry, 1989 (*J. Inorg. Biochem.* **1989**, *36*, 223, Abstr G059).
(17) Krüger, H.-J.; Holm, R. H. *Inorg. Chem.* **1989**, *28*, 1148.
(18) Kumar, M.; Day, R. O.; Colpas, G. J.; Maroney, M. J. *J. Am. Chem. Soc.* **1989**, *111*, 5974.
(19) (a) Dance, I. G. *Polyhedron* **1987**, *5*, 1037. (b) Blower, P. J.; Dilworth, J. R. *Coord. Chem. Rev.* **1987**, *76*, 121.
(20) Ockels, W.; Römer, A.; Budzikiewicz, H.; Korth, H.; Pulverer, G. *Tetrahedron Lett.* **1978**, 3341.
(21) (a) Hildebrand, U.; Lex, J.; Taraz, K.; Winkler, S.; Ockels, W.; Budzikiewicz, H. *Z. Naturforsch.* **1984**, *39B*, 1607. (b) Note added in proof: We have recently become aware of the structural determination of $(Et_4N)[Co(pdtc)_2]$: Hildebrand, U. H. W.; Lex, J. *Z. Naturforsch.* **1989**, *44b*, 475. Metric features are similar to those reported here. Our results do not substantiate the claim of these investigators, based on spectroscopic results, that $[Ni(pdtc)_2]^{1-}$ is tetrahedral.
(22) Baucom, E. I.; Drago, R. S. *J. Am. Chem. Soc.* **1971**, *93*, 6469.
(23) Drago, R. S.; Baucom, E. I. *Inorg. Chem.* **1972**, *11*, 2064.
(24) Bemtgen, J.-M.; Gimpert, H.-R.; von Zelewsky, A. *Inorg. Chem.* **1983**, *22*, 3576.
(25) Hildebrand, U.; Ockels, W.; Lex, J.; Budzikiewicz, H. *Phosphorous Sulfur* **1983**, *16*, 361.

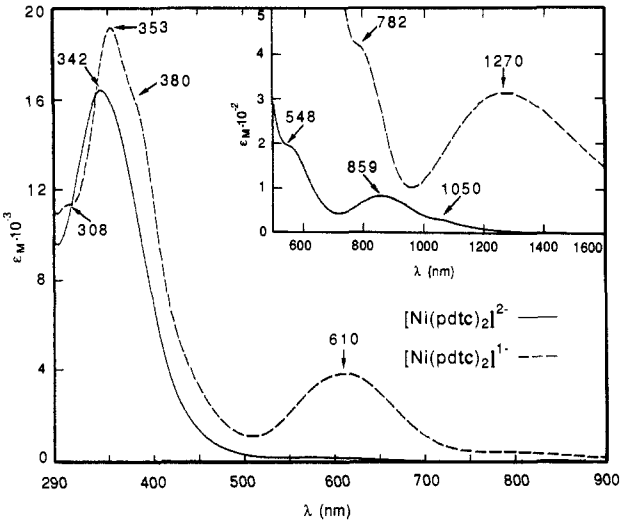

Figure 1. UV/vis/NIR absorption spectra of $[Ni(pdtc)_2]^{2-}$ and $[Ni(pdtc)_2]^{1-}$ in DMF solutions; band maxima and shoulders are indicated.

(DMF): λ_{max} (ϵ_M) 376 nm (20 600), 480 (2350), 580 (sh, 169). IR (KBr): 1610, 1577, 1490, 1255, 1175, 928, 825, 752 cm^{-1} (strong bands only).

The $(Ph_3PCH_2Ph)^+$ salt, which was useful for X-ray crystallography, was obtained as in the preceding preparation.

Collection and Reduction of X-ray Data. An acceptable crystal of $(Et_4N)_2[Ni(pdtc)_2]$ (A) was cut from a larger, dark brown crystal obtained by recrystallization from ethanol. Large, dark green crystals of $(Ph_3PCH_2Ph)[Ni(pdtc)_2]$ (B) were obtained by slow diffusion of ether into an acetone solution at 4 °C. A suitable crystal was cut from a larger crystal. Orange-brown single crystals of $(Ph_3PCH_2Ph)[Co(pdtc)_2]$ (C) were grown by the method used for B. Data collections were carried out at ambient temperature on a Nicolet P3F automated four-circle diffractometer using graphite-monochromatized Mo Kα radiation. The unit cell parameters and final orientation matrices were obtained from least-squares refinement of 25 machine-centered reflections in the range $20° \leq 2\theta \leq 25°$. Three standard reflections measured every 123 reflections indicated no decay of the crystals during data collections. The data sets were processed with the programs XTAPE of the SHELXTL program package (Nicolet XRD Corporation, Madison, WI 53711), and empirical absorption corrections were applied using the program PSICOR. The systematic absences hkl ($h + k = 2n + 1$), $h0l$ ($h,l = 2n + 1$), and $0k0$ ($k = 2n + 1$) for compound A are consistent with monoclinic space groups Cc (No. 9) and $C2/c$ (No. 15). Simple E statistics favored the centrosymmetric space group. Subsequent successful solution and refinement of the structure proved this choice to be correct. For compounds B and C, which are isomorphous, the systematic absences $h0l$ ($h + l = 2n + 1$) and $0k0$ ($k = 2n + 1$) uniquely determine the space group $P2_1/n$ (No. 14). Crystallographic data are summarized in Table I.

Structure Solution and Refinement. The non-hydrogen atoms in the three structures were located by direct methods (SHELXTL) or by Fourier difference maps using the program CRYSTALS. Atom scattering factors were taken from a standard source.[26] In compound A, the Ni atom is located on a special position of a twofold rotation axis (0, $-y$, 0.75). During refinement, the x and z positions were fixed, and in the anisotropic refinement the temperature factors $U(12)$ and $U(23)$ were set to zero. For compound A, the asymmetric unit consists of one ligand, one-half Ni, and one cation. In compounds B and C, the asymmetric unit consists of one anion and one cation. Isotropic refinement converged at 9.9% (A), 13.4% (B), and 12.0% (C). In the final stages of anisotropic refinement, hydrogen atoms were introduced at 0.98 Å from the bonded carbon atoms with an isotropic thermal parameter of 0.1 $Å^2$. Final difference Fourier maps showed no peaks larger than 0.22 (A), 0.27 (B), and 0.29 e/$Å^3$ (C). Final R factors are given in Table I.[27]

Other Physical Measurements. Absorption spectra were recorded on a Varian 2390 and a Perkin-Elmer Lambda 4C spectrophotometer. ^1H NMR spectra were obtained with a Bruker AM-500 spectrometer. Solution susceptibilities were measured by the usual NMR method[28] and calculated with use of reported Me_2SO susceptibility.[29] Infrared spectra were recorded on a Nicolet FT-IR 43 instrument. EPR spectra were determined with a Varian E Line spectrometer operating at X-band frequencies. Solutions of electrochemically generated $[Ni(pdtc)_2]^{1-}$ and $[Ni(dapo)_2]^{1-}$ and of $(Et_4N)[Ni(pdtc)_2]$ were prepared shortly before measurement and frozen in liquid nitrogen prior to use. Electrochemical measurements were made with standard PAR instrumentation. In cyclic voltammetric experiments, solutions ca. 1 mM in complex with the supporting electrolytes 0.2 M Bu_4NClO_4 (DMF THF, MeCN, propylene carbonate), 0.2 M LiCl (EtOH), and 0.2 M KCl and 0.05 M buffer (water) were used. Potentials were measured at 298 K vs a SCE reference electrode by using a Pt foil or a glassy carbon working electrode. Measured potentials were not corrected for junction potentials. Under the conditions employed, the potentials (V) of the ferrocinium/ferrocene couple were 0.48 (DMF, CH_2Cl_2), 0.40 (MeCN), 0.42 (EtOH), 0.54 (THF), and 0.39 (propylene carbonate). Coulometric experiments were performed with a Pt gauze electrode and a PAR Model 179 digital coulometer.

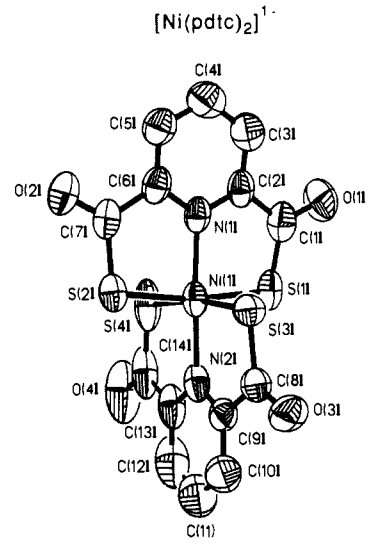

Figure 2. Structure of $[Ni(pdtc)_2]^{1-}$ showing overall stereochemistry with 50% probability ellipsoids and the atom numbering scheme.

Results and Discussion

In this investigation, two sets of nickel complexes are of primary interest, $[Ni(pdtc)_2]^z$ (**3**, **4**) and $[Ni(dapo)_2]^z$ (**5**–**7**). Of these,

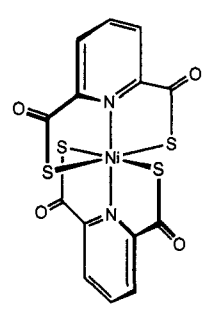

z = 2- (**3**), 1- (**4**)

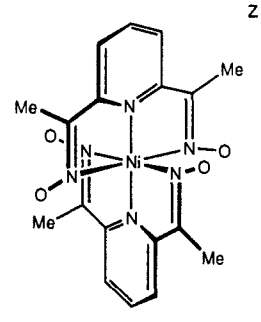

z = 2- (**5**), 1- (**6**), 0 (**7**)

$[Ni(dapo)_2]^{0,2-}$ have been previously examined,[22] and the octahedral structure of $[Ni(dapo)_2]$ has been demonstrated crystallographically.[30] The only complex of ligand **1** that has been previously reported is $[Fe(pdtc)_2]^{1-}$.[21a]

Synthesis and Properties of $[Ni(pdtc)_2]^{2-,1-}$. The Et_4N^+ salt of $[Ni(pdtc)_2]^{2-}$ was simply prepared by the reaction of $Ni(OAc)_2$ with a slight excess of the ligand in an ethanolic Et_4NOH solution. Upon recrystallization from ethanol, the compound can be obtained as beautiful dark brown needles. It is quite soluble in MeOH, MeCN, DMF, and water. When exposed to air, $[Ni(pdtc)_2]^{2-}$ is stable for days in the solid state and in solution. An octahedral structure in solution is supported by the magnetic

(26) Cromer, D. T.; Waber, J. T. *International Tables for X-Ray Crystallography*; Kynoch Press: Birmingham, England, 1974.
(27) See the paragraph at the end of this article concerning supplementary material available.
(28) Live, D. H.; Chan, S. I. *Anal. Chem.* **1970**, *42*, 791.
(29) Gerger, W.; Mayer, U.; Gutmann, V. *Monatsh. Chem.* **1977**, *108*, 417.
(30) Sproul, G.; Stucky, G. D. *Inorg. Chem.* **1973**, *12*, 2898.

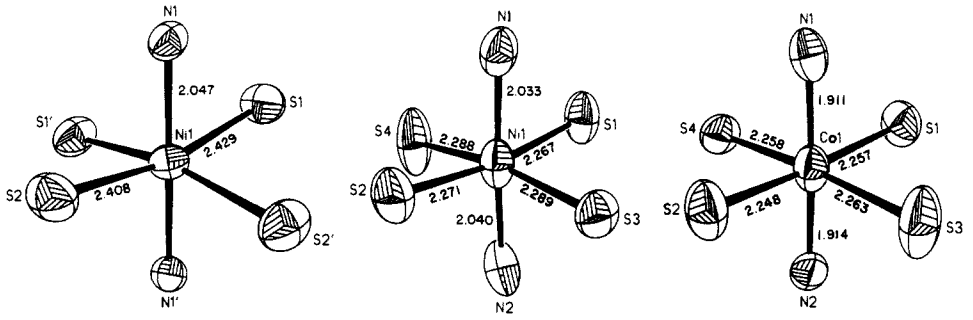

$[Ni(pdtc)_2]^{2-}$

S1-Ni1-S2 = 167.1
N1-Ni1-N1' = 177.3

$[Ni(pdtc)_2]^{-}$

S1-Ni1-S2 = 170.3
S3-Ni1-S4 = 169.8
N1-Ni1-N2 = 175.6

$[Co(pdtc)_2]^{-}$

S1-Co1-S2 = 174.5
S3-Co1-S4 = 174.8
N1-Co1-N2 = 177.4

Figure 3. Coordination units of $[Ni(pdtc)_2]^{2-}$, $[Ni(pdtc)_2]^{1-}$, and $[Co(pdtc)_2]^{1-}$, showing 50% ellipsoids, the atom numbering scheme, and selected bond distances and angles. Primed and unprimed atoms are related by a twofold axis.

Table II. Selected Interatomic Distances (Å) for $[Ni(pdtc)_2]^{2-}$ (A), $[Ni(pdtc)_2]^{1-}$ (B), and $[Co(pdtc)_2]^{1-}$ (C)

distance	A	B	C
M-S(1)	2.4290 (8)	2.267 (1)	2.257 (1)
M-S(2)	2.4079 (9)	2.271 (1)	2.248 (1)
M-S(3)		2.289 (1)	2.263 (1)
M-S(4)		2.288 (1)	2.258 (1)
M-N(1)	2.047 (2)	2.033 (3)	1.911 (4)
M-N(2)		2.040 (4)	1.914 (4)
S(1)-C(1)	1.705 (3)	1.715 (5)	1.718 (5)
S(2)-C(7)	1.701 (3)	1.719 (5)	1.705 (6)
S(3)-C(8)		1.723 (4)	1.708 (7)
S(4)-C(14)		1.750 (7)	1.713 (5)
N(1)-C(2)	1.336 (3)	1.331 (5)	1.356 (5)
N(1)-C(6)	1.343 (3)	1.346 (5)	1.354 (6)
N(2)-C(9)		1.347 (5)	1.352 (6)
N(2)-C(13)		1.344 (5)	1.363 (6)
O(1)-C(1)	1.231 (3)	1.227 (5)	1.226 (5)
O(2)-C(7)	1.233 (3)	1.233 (5)	1.225 (6)
O(3)-C(8)		1.225 (5)	1.230 (6)
O(4)-C(14)		1.220 (6)	1.229 (5)
C(1)-C(2)	1.515 (4)	1.507 (6)	1.498 (7)
C(6)-C(7)	1.505 (4)	1.505 (6)	1.515 (6)
C(8)-C(9)		1.485 (6)	1.493 (8)
C(13)-C(14)		1.480 (8)	1.487 (6)

Table III. Selected Interatomic Angles (deg) for $[Ni(pdtc)_2]^{2-}$ (A), $[Ni(pdtc)_2]^{1-}$ (B), and $[Co(pdtc)_2]^{1-}$ (C)

angle	A	B	C
S(2)-M-S(1)	167.07 (2)	170.33 (5)	174.50 (6)
S(3)-M-S(1)	91.68 (3)	91.22 (4)	89.53 (5)
S(3)-M-S(2)	90.78 (5)	90.91 (4)	89.33 (5)
S(4)-M-S(1)	88.75 (5)	89.32 (5)	90.75 (5)
S(4)-M-S(2)		90.24 (5)	90.88 (5)
S(4)-M-S(3)		169.83 (6)	174.77 (7)
N(1)-M-S(1)	83.62 (6)	85.1 (1)	87.3 (1)
N(1)-M-S(2)	83.53 (6)	85.5 (1)	87.4 (1)
N(1)-M-S(3)	94.59 (6)	91.14 (9)	94.9 (1)
N(1)-M-S(4)	98.30 (6)	99.0 (1)	90.3 (1)
N(2)-M-S(1)		94.32 (9)	93.7 (1)
N(2)-M-S(2)		95.27 (9)	91.7 (1)
N(2)-M-S(3)		84.5 (1)	87.5 (1)
N(2)-M-S(4)		85.3 (1)	87.2 (1)
N(2)-M-N(1)	177.3 (1)	175.6 (1)	177.4 (2)
C(1)-S(1)-M	98.0 (1)	99.9 (2)	98.4 (2)
C(7)-S(2)-M	98.6 (1)	99.6 (2)	99.0 (2)
C(8)-S(3)-M		100.0 (1)	97.9 (2)
C(14)-S(4)-M		99.1 (2)	98.7 (2)
C(2)-N(1)-M	120.6 (2)	120.1 (3)	121.0 (3)
C(6)-N(1)-M	120.3 (2)	120.4 (3)	120.5 (3)
C(6)-N(1)-C(2)	119.0 (2)	119.2 (4)	118.4 (4)
C(9)-N(2)-M		120.5 (3)	120.6 (4)
C(13)-N(2)-M		120.3 (4)	120.4 (3)
C(13)-N(2)-C(9)		119.2 (4)	119.0 (5)
O(1)-C(1)-S(1)	124.5 (3)	123.2 (4)	124.4 (4)
C(2)-C(1)-S(1)	118.1 (2)	117.1 (4)	116.1 (3)
C(2)-C(1)-O(1)	117.4 (3)	119.6 (5)	119.5 (5)
C(1)-C(2)-N(1)	119.4 (2)	117.0 (4)	116.8 (4)
C(7)-C(6)-N(1)	119.3 (2)	116.3 (4)	116.9 (5)
O(2)-C(7)-S(2)	125.2 (3)	123.5 (4)	125.3 (4)
C(6)-C(7)-S(2)	117.7 (2)	117.8 (3)	115.6 (4)
C(6)-C(7)-O(2)	117.1 (3)	118.7 (4)	119.0 (5)
O(3)-C(8)-S(3)		123.5 (3)	124.8 (6)
C(9)-C(8)-S(3)		117.4 (3)	117.2 (4)
C(9)-C(8)-O(3)		119.1 (4)	118.0 (7)
C(8)-C(9)-N(2)		117.3 (4)	116.8 (5)
C(14)-C(13)-N(2)		117.6 (5)	117.4 (4)
O(4)-C(14)-S(4)		122.7 (6)	124.5 (4)
C(13)-C(14)-S(4)		117.6 (4)	116.1 (3)
C(13)-C(14)-O(4)		119.7 (7)	119.4 (4)

moment of 3.13μ_B in Me_2SO and the absorption spectrum in DMF shown in Figure 1. Features at 1050 and 859 nm correspond to splitting of the octahedral ν_1 band ($^3A_{2g} \rightarrow {}^3T_{2g}$) in lower symmetry. The ν_2 band ($^3A_{2g} \rightarrow {}^3T_{1g}$) appears as a shoulder at 548 nm. The 3-H and 4-H resonances occur at 65.8 and 20.0 ppm, respectively, indicative of large negative contact shifts arising from spin delocalization through σ bonds. Similar shifts have been observed for $[Ni(dapo)_2]^{2-}$[22] and other Ni(II) complexes with pyridine-type ligands.[31]

Oxidation of $[Ni(pdtc)_2]^{2-}$ with iodine in methanol afforded dark green $[Ni(pdtc)_2]^{1-}$, which was isolated in 85% yield as its Et_4N^+ salt. This compound is soluble in acetone, DMF, and Me_2SO in which it is stable for at least 1 day under anaerobic conditions. The magnetic moment of 1.79μ_B in Me_2SO is consistent with a low-spin d^7 configuration. The absorption spectrum (Figure 1) is dominated by the intense LMCT band at 610 nm, which accounts for the green color of the complex. An absorption of similar origin has been observed at 718 nm for a Ni(III) amidatethiolate species.[15] Certain other electronic properties of $[Ni(pdtc)_2]^{1-}$ are described below.

Structures of $[Ni(pdtc)_2]^{2-,1-}$ and $[Co(pdtc)_2]^{1-}$. Crystals of the $(Ph_3PCH_2Ph)^+$ salts of the two monoanionic complexes are isomorphous (Table I). The configurations of the three complexes are very similar and can be represented by that of $[Ni(pdtc)_2]^{1-}$, shown in Figure 2. Coordination spheres are depicted in Figure 3. Selected interatomic distances and angles are contained in Tables II and III, respectively. $[Ni(pdtc)_2]^{2-}$ has crystallographically imposed C_2 symmetry. Comparisons of certain structural features among Ni, Co, and Fe complexes are presented in Table IV.[21b]

The three complexes examined here have meridionally coordinated, essentially planar pdtc ligands, the dihedral angles of which are close to 90°. The dihedral angle between the ligand plane and the least-squares MS_4 plane is 90.4° in $[Ni(pdtc)_2]^{2-}$.

(31) (a) Horrocks, W. D.; Johnston, D. L. *Inorg. Chem.* **1971**, *10*, 1835. (b) Happe, J. A.; Ward, R. L. *J. Chem. Phys.* **1963**, *39*, 1211.

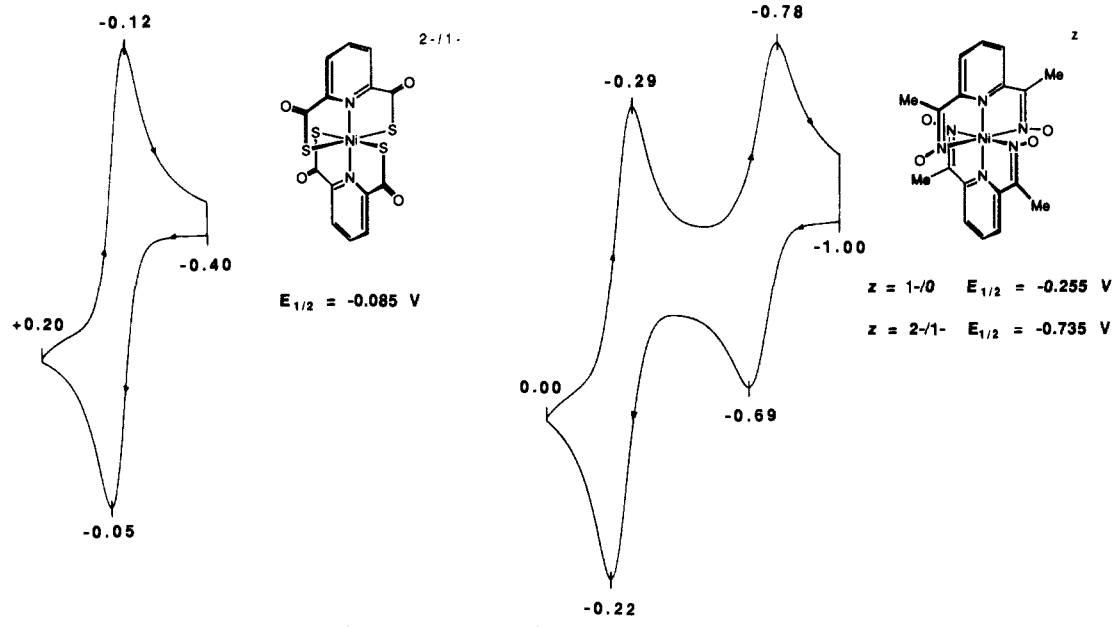

Figure 4. Cyclic voltammograms of $[Ni(pdtc)_2]^{2-/1-}$ and $[Ni(dapo)_2]^{2-/1-/0}$ at a Pt foil electrode in DMF solutions; peak and half-wave potentials vs SCE are indicated.

Table IV. Comparative Structural Properties of $[M(pdtc)_2]^{2-,1-}$ Complexes[a]

property	$[Ni(pdtc)_2]^{2-}$	$[Ni(pdtc)_2]^{1-}$	$[Co(pdtc)_2]^{1-}$	$[Fe(pdtc)_2]^{1-}$[b]
S	1	$^1/_2$	0	$^1/_2$
Shannon radius,[c] Å	0.83	0.74	0.685	0.69
M–S	2.418	2.279	2.257	2.280[e]
M–N	2.047	2.037	1.913	1.944
S–M–S	167.1	170.1	174.6	171.9
S–M–N	83.6	85.1	87.4	86.2
L/L'[f]	92.1	85.6	85.5	95.3
$\Delta(MS_4)$[d]				
M	0.000	−0.005	0.001	−0.004
S_1	0.273	−0.196	−0.104	0.159
S_2	0.270	−0.196	−0.104	0.153
S_3	−0.273	0.195	0.105	−0.153
S_4	−0.270	0.200	0.103	−0.155

[a] Mean values of distances (Å) and angles (deg). [b] Data from ref 21a. [c] Shannon, R. D. *Acta Crystallogr.* **1976**, *A32*, 751. [d] Atom displacements from least-squares MS_4 planes. [e] If one Fe–S distance, lengthened because of pyH^+–carbonyl hydrogen bonding, is neglected, the mean bond distance is 2.274 Å. [f] Dihedral angle between ligand planes.

For reasons unclear, one ligand is tipped toward this plane more than the other in $[Ni(pdtc)_2]^{1-}$ (82.0°) and $[Co(pdtc)_2]^{1-}$ (84.5°). Deviations of sulfur atoms from the MS_4 planes are largest with $[Ni(pdtc)_2]^{2-}$ (±0.27 Å, Table IV). Of the three established modes of binding of monothiocarboxylates to Ni(II), monodentate[32] (**8**),

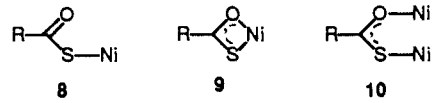

8 **9** **10**

bidentate mononuclear[33] (**9**), and bidentate binuclear[34] (**10**), the first of these occurs with the two nickel complexes as well as with $[Co(pdtc)_2]^{1-}$ and $[Fe(pdtc)_2]^{1-}$.[21] The coordination units closely approach tetragonally distorted octahedra. In an overall sense, the three structures resemble those of $[Fe(pdtc)_2]^{1-}$[21a] and $[Ni(dapo)_2]$.[30]

The mean Ni–S distance of 2.418 Å in $[Ni(pdtc)_2]^{2-}$ falls into the range of six-coordinate Ni(II)–S bond lengths observed with high-spin complexes of anionic sulfur ligands, including thiolates,[35] mono-[32] and dithiocarboxylates,[36] monothiocarbamates,[37] xanthates,[38] and thiosemicarbazonates.[39] Similarly, the Ni–N distance of 2.047 Å is consistent with earlier values for molecules in which a pyridyl group is part of a multidentate ligand.[35b,40] The only indication of possible strain in the coordination sphere and ligand is the S(1)–Ni–S(2) angle of 167.1 (2)°. This occurs because the five-membered chelate rings are slightly too small to accommodate four sulfur atoms in the plane with unexceptional, but for this particular complex not necessarily optimal, Ni–S and Ni–N distances. As seen in Table IV, out-of-plane sulfur atom displacements decrease and S–M–S angles increase as the size of the metal ion decreases.

Relative to $[Ni(pdtc)_2]^{2-}$, the mean Ni–N and Ni–S distances in $[Ni(pdtc)_2]^{1-}$ have decreased by 0.01 and 0.14 Å, respectively. This is the effect expected as a consequence of metal-centered oxidation and has been observed in four previous pairs of Ni(II)/Ni(III) complexes with six-coordinate structures.[41-44] None

(32) (a) Ramalingam, K.; Aravamudan, G.; Seshasayee, M.; Verghese, B. *Acta Crystallogr.* **1987**, *C43*, 471. (b) Ruble, J. R.; Seff, K. *Acta Crystallogr.* **1972**, *B28*, 1272.

(33) (a) Musaev, F. N.; Movsumov, E. M.; Mamedov, K. S.; Amiraslanov, I. R.; Magerramov, A. I.; Shnulin, A. N. *J. Struct. Chem.* **1977**, *18*, 865. (b) Borel, M. M.; Geffrouais, A.; Ledesert, M. *Acta Crystallogr.* **1976**, *B32*, 2385.

(34) (a) Melson, G. A.; Greene, P. T.; Bryan, R. F. *Inorg. Chem.* **1970**, *9*, 1116. (b) Melson, G. A.; Crawford, N. P.; Geddes, B. J. *Inorg. Chem.* **1970**, *9*, 1123.

(35) (a) Osakada, K.; Yamamoto, T.; Yamamoto, A.; Takenaka, A.; Sasada, Y. *Acta Crystallogr.* **1984**, *C40*, 85. (b) Rosenfield, S. G.; Berends, H. P.; Gemini, L.; Stephan, D. W.; Mascharak, P. K. *Inorg. Chem.* **1987**, *26*, 2792.

(36) (a) Fackler, J. P., Jr.; Del Niera P., R.; Campana, C.; Trzcinska-Bancroft, B. *J. Am. Chem. Soc.* **1984**, *106*, 7883. (b) Bonamico, M.; Dessy, G.; Fares, V.; Flamini, A.; Scaramuzza, L. *J. Chem. Soc., Dalton Trans.* **1976**, 1743.

(37) Bereman, R. D.; Baird, D. M.; Dorfman, J. D.; Bordner, J. *Inorg. Chem.* **1982**, *21*, 2365.

(38) (a) Edwards, A. J.; Hoskins, B. F.; Winter, G. *Aust. J. Chem.* **1986**, *39*, 1983. (b) Gable, R. W.; Hoskins, B. F.; Winter, G. *Inorg. Chim. Acta* **1985**, *96*, 151. (c) Bizilj, K.; Hardin, S. G.; Hoskins, B. F.; Oliver, P. J.; Tiekink, E. R. T.; Winter, G. *Aust. J. Chem.* **1986**, *39*, 1035.

(39) (a) Mathew, M.; Palenik, G. J. *J. Am. Chem. Soc.* **1969**, *91*, 6310. (b) Clark, G. R.; Palenik, G. J. *Cryst. Struct. Commun.* **1980**, *9*, 449.

(40) Masuko, A.; Nomura, T.; Saito, Y. *Bull. Chem. Soc. Jpn.* **1967**, *40*, 511.

(41) $[Ni(tacn)_2]^{2+,3+}$ (tacn = 1,4,7-triazacyclononane): (a) Zompa, L. J.; Margulis, T. N. *Inorg. Chim. Acta* **1978**, *28*, L157. (b) Wieghardt, K.; Walz, W.; Nuber, B.; Weiss, J.; Ozarowski, A.; Stratemeier, H.; Reinen, D. *Inorg. Chem.* **1986**, *25*, 1650.

(42) $[Ni([14]aneN_4)Cl_2]^{0,1+}$ ([14]aneN$_4$ = 1,4,8,11-tetraazacyclotetradecane): (a) Bosnich, B.; Mason, R.; Pauling, P. J.; Robertson, G. B.; Tobe, M. L. *Chem. Commun.* **1968**, 97. (b) Ito, T.; Sugimoto, M.; Toriumi, K.; Ito, H. *Chem. Lett.* **1981**, 1477.

(43) $[Ni(tacnta)]^{1-,0}$ (tacnta = 1,4,7-triazacyclononane-*N*,*N'*,*N''*-triacetate): van der Merwe, M. J.; Boeyens, J. C. A.; Hancock, R. D. *Inorg. Chem.* **1983**, *22*, 3489.

of these involve sulfur ligands. The Ni–S distance of the oxidized complex is very close to that in the diamagnetic Ni(IV) complex $[Ni(S_2CNEt_2)_3]^{1+}$ (2.261 Å[45]) and ~0.14 Å longer than in the dithiolenes $[Ni(S_2C_2R_2)_2]^{1-}$.[46] The dithiolenes are nonclassical species that have Ni(III) ground-state character,[47] but are extensively delocalized and are not directly pertinent to $[Ni(pdtc)_2]^{1-}$.

The structure of $[Co(pdtc)_2]^{1-}$ is metrically similar to that of $[Ni(pdtc)_2]^{1-}$, except that the mean Co–N distance is 0.124 Å shorter than the corresponding distance in the latter complex. We shall return to some comparative structural features of these three complexes. For now, we observe that, other than possibly the 3.0° difference in S–Ni–S angles and attendant ca. 0.07 Å difference in displacements of sulfur atoms from the NiS_4 planes, there is no specific *structural* feature of the ligand that favors Ni(III) over Ni(II), or conversely.

Electron-Transfer Reactions. (a) $[Ni(pdtc)_2]^z$. The redox couple 1 is established by the cyclic voltammogram in Figure 4 and by

$$[Ni(pdtc)_2]^{2-} \rightleftharpoons [Ni(pdtc)_2]^{1-} + e^- \qquad (1)$$

coulometry, as well as by chemical oxidation. The peak-to-peak separation ΔE_p = 70 mV at scan rate ν = 20 mV/s and 90 mV at ν = 200 mV/s, peak current function $i_p/\nu^{1/2}$ is independent of ν, and $i_{pa}/i_{pc} \approx 1$ at all scan rates. Coulometric oxidation at +0.12 V resulted in the passage of an average of 0.98F in three determinations. Reduction at −0.29 V caused transfer of 97% of the charge passed in oxidation, indicating very little, if any, decay of the oxidized species over the 30-min period of the experiment. Thus, couple 1 is an electrochemically quasi-reversible, chemically reversible process with $E_{1/2}$ = −0.085 V in DMF solution.

(b) $[Ni(dapo)_2]^z$. With the establishment of reaction 1 and isolation of $[Ni(pdtc)_2]^{1-}$, the question arose as to why previous attempts to produce $[Ni(dapo)_2]^{1-}$ from either $[Ni(dapo)_2]^{2-}$ or $[Ni(dapo)_2]$ were unsuccessful. Similar to prior experiences with this and other oximate ligands,[14,22] we encountered difficulties in isolating a pure sample of the (assumed) Ni(III) complex by chemical means. While the electrochemical behavior of $[Ni(dapo)_2]$ at a Pt foil electrode in DMF afforded a quasi-reversible reduction at −0.255 V by cyclic voltammetry, a second reductive process was complicated by adsorption. Baucom and Drago[22] had noted difficulties due to "surface reactions" in their electrochemical experiments (conditions unspecified).

These problems can be avoided by starting with $[Ni(dapo)_2]^{2-}$. The three-membered electron-transfer series 2 with $E_{1/2}$ = −0.735

$$[Ni(dapo)_2]^{2-} \underset{+e^-}{\overset{-e^-}{\rightleftharpoons}} [Ni(dapo)_2]^{1-} \underset{+e^-}{\overset{-e^-}{\rightleftharpoons}} [Ni(dapo)_2] \qquad (2)$$

(1−/2−) and −0.255 V (0/1−) follows from the voltammogram in Figure 4. The properties of the two steps are essentially the same as those of the voltammogram of reaction 1. However, the coulometry is not as well-behaved, 0.84 and 1.73F being consumed in the first step and in the full oxidation of the Ni(II) complex. The reactions are quite sluggish at a Pt surface, and some decomposition may have ensued during electrolysis.

The first oxidation reaction was also followed by spectrophotometry, as seen in Figure 5. The red Ni(II) complex has its octahedral ν_2 d–d band near 640 nm.[22] The green color of $[Ni(dapo)_2]^{1-}$ arises from the LMCT band at 649 nm, which must be the counterpart of the 610-nm band of $[Ni(pdtc)_2]^{1-}$. The spectrum of bluish-green $[Ni(dapo)_2]$ in DMF is quite similar to that reported for the solid compound.[22]

Ground States of Oxidized Complexes. (a) $[Ni(pdtc)_2]^{1-}$. The metal-centered nature of the oxidation of the Ni(II) complex and the ground state of $[Ni(pdtc)_2]^{1-}$ have been demonstrated by electronic and structural properties. In frozen DMF solution, the

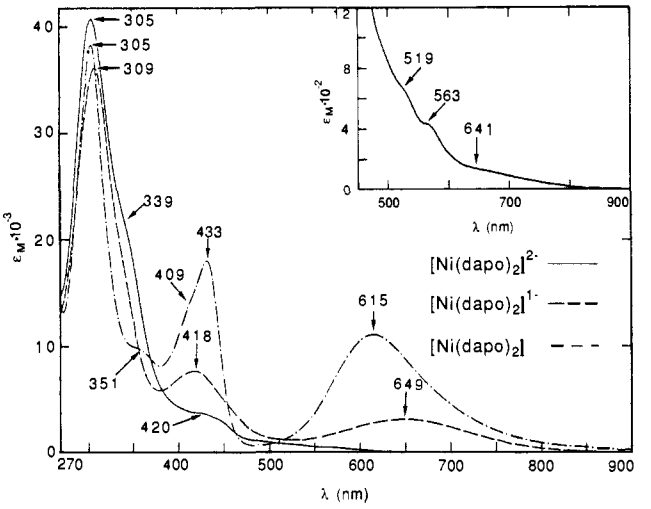

Figure 5. UV/vis absorption spectra [λ_{max} (ϵ_M)] of $Na_2[Ni(dapo)_2]$ [305 nm (41 000), 339 (sh, 22 800), 420 (sh, 4010), 519 (sh, 696), 563 (sh, 431), 641 (sh, 162)]; electrochemically generated $[Ni(dapo)_2]^{1-}$ [309 nm (36 400), 418 (7670), 649 (3120)]; and $[Ni(dapo)_2]$ in DMF solutions. $[Ni(dapo)_2]^{1-}$ was generated at −0.50 V and the spectrum was recorded in the presence of 0.1 M Bu_4NClO_4; extinction coefficients are ca. 15% too low (based on coulometry). Because of the low solubility of $[Ni(dapo)_2]$ in DMF, the spectrum conveys relative absorbances only.

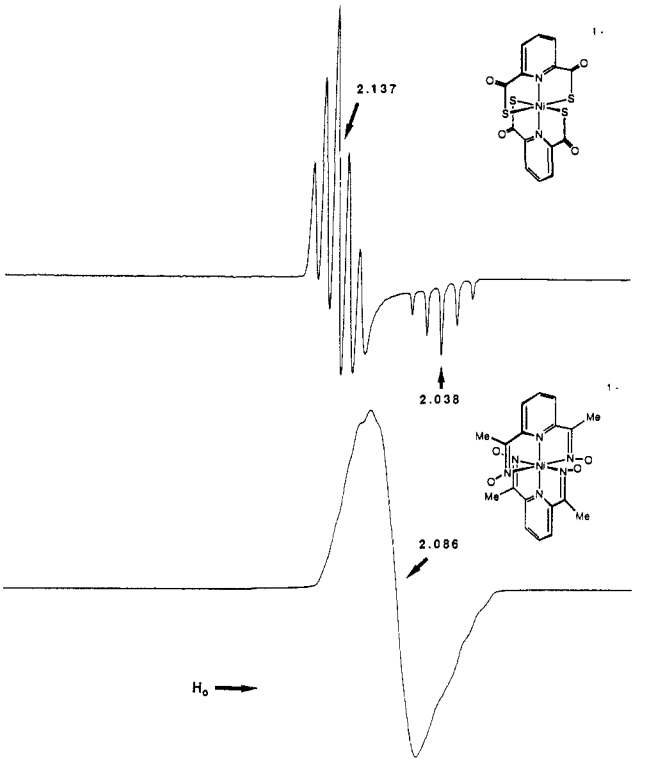

Figure 6. X-band EPR spectra of $(Et_4N)[Ni(pdtc)_2]$ and electrochemically generated $[Ni(dapo)_2]^{1-}$ in DMF solutions at 100 K; apparent g values are indicated.

EPR spectrum of the monoanion in Figure 6 consists of an axial signal with $g_\perp$ = 2.137 and $g_\parallel$ = 2.038. Hyperfine splitting from ^{14}N is particularly well-resolved, with $a_\parallel^N$ = 21.1 G and $a_\perp^N$ = 16.2 G. When examined in fluid dichloromethane solution at ambient temperature, the spectrum in Figure 7 has $\langle g \rangle$ = 2.103 and $\langle a^N \rangle$ = 17 ± 0.5 G. Enrichment of the complex in 86.4 atom % ^{61}Ni ($I = {}^3/_2$) affords resolved hyperfine splittings with $\langle a^{Ni} \rangle$ = 22 ± 1 G. Parameters were obtained by spectral simulations (not shown). Values of $\langle g \rangle$ and $\langle a^{Ni} \rangle$ together with the anisotropy of the signal are consistent with a Ni(III) formulation. Further, $g_\perp > g_\parallel$ is consistent only with a tetragonally distorted geometry and the $^2A_{1g}[(d_{z^2})^1]$ ground state.[47] This is the expected result

(44) $[Ni(bpy)_3]^{2+,3+}$ (bpy = 2,2′-bipyridyl): (a) Wada, A.; Sakabe, N.; Tanaka, J. *Acta Crystallogr.* **1976**, *B32*, 1121. (b) Szalda, D. J.; Macartney, D. H.; Sutin, N. *Inorg. Chem.* **1984**, *23*, 3473.

(45) Fackler, J. P., Jr.; Avdeef, A.; Fischer, R. G., Jr. *J. Am. Chem. Soc.* **1973**, *95*, 774.

(46) Mahadevan, C.; Seshasayee, M.; Kuppusamy, P.; Manoharan, P. T. *J. Crystallogr. Spectrosc. Res.* **1984**, *14*, 179, and references therein.

(47) Maki, A. H.; Edelstein, N.; Davison, A.; Holm, R. H. *J. Am. Chem. Soc.* **1964**, *86*, 4580.

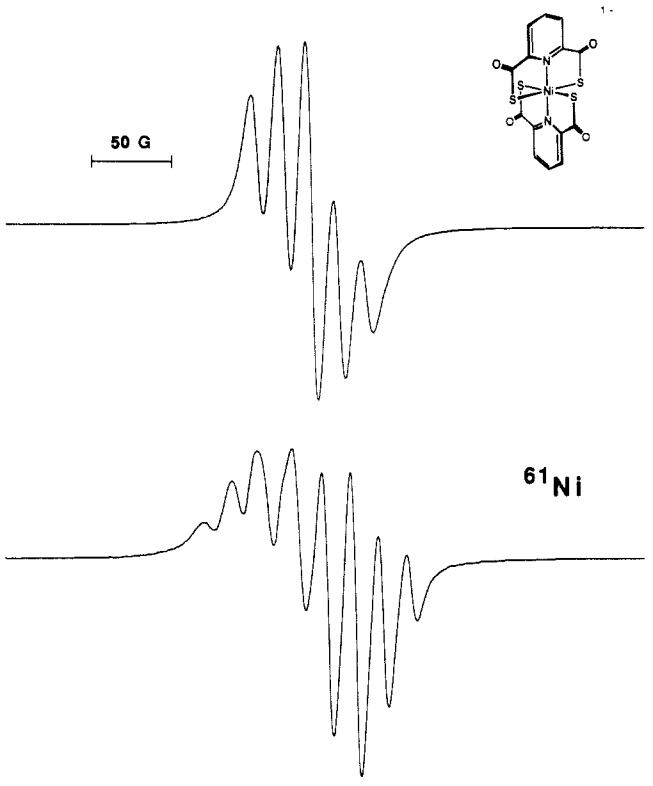

Figure 7. X-band EPR spectra of $[Ni(pdtc)_2]^{1-}$ (upper) and $[^{61}Ni(pdtc)_2]^{1-}$ (lower, 86.4 atom % enrichment) in dichloromethane solutions at 298 K. These species were generated in ca. 1 mM solutions containing 0.1 M Bu_4NClO_4 at a Pt gauze electrode maintained at a potential of +0.115 V.

for a complex with a strong in-plane ligand field, such as is afforded by four anionic sulfur ligands. However, that $g_\parallel > 2$ indicates some mixing of excited configurations into the ground state. In terms of resolution and splittings, a strikingly similar spectrum is found for $[Ni(CN)_4(NH_3)_2]^{1-}$ with $a_\parallel$ and $a_\perp$ values of 24.5 and 18.3 G and the unpaired electron in the d_{z^2} orbital.[48] For the related species $[Ni(CN)_4(OH_2)_2]^{1-}$ with the same ground state, ^{61}Ni hyperfine splitting is observed, with $a_\parallel$ = 43 G.[48,49]

With reference to Table IV, the decrease in mean Ni–S distances and essentially constant Ni–N distances upon passing from $[Ni(pdtc)_2]^{2-}$ to $[Ni(pdtc)_2]^{1-}$ is consistent with the removal of an antibonding electron and a change from the $(d_{z^2})^1(d_{x^2-y^2})^1$ to the $(d_{z^2})^1$ ground-state configuration. For the pairs $[Ni(tacn)_2]^{3+,2+}$[41] and $[Ni([14]ane)Cl_2]^{1+,0}$,[42] whose oxidized members have the $(d_{z^2})^1$ configuration, related bond length changes occur. For example, in the latter pair, the equatorial Ni–N distances decrease more than the axial Ni–Cl distances upon oxidation. The Co–S and Co–N bond distances of diamagnetic $[Co(pdtc)_2]^{1-}$, when compared to corresponding values in sterically unconstrained octahedral Co(III) complexes,[50,51] are unexceptional. They are shorter than the bonds in $[Ni(pdtc)_2]^{1-}$, in part because of the smaller low-spin octahedral radius of Co(III). However, that the Co–N distance is also 0.12 Å shorter whereas the Co–S bond is only 0.02 Å shorter is indicative of the $(d_{z^2})^1$ configuration in the Ni(III) complex. No strikingly unequal bond length differences occur when $[Co(pdtc)_2]^{1-}$ and low-spin $[Fe(pdtc)_2]^{1-}$[21] are compared. Their electron configurations differ by population of one electron in the approximately nonbonding t_{2g}-type orbitals. These arguments, while simple, are effective in establishing the ground state of $[Ni(pdtc)_2]^{1-}$.

Table V. Solvent Dependence of Redox Potentials

solvent	$E_{1/2}$, V[a]		
	$[Ni(pdtc)_2]^{1-/2-}$	$[Ni(dapo)_2]^{1-/2-}$	$[Ni(dapo)_2]^{0/1-}$
H_2O, pH 10	+0.145 (90)[b]	+0.055 (190)[b]	+0.215 (70)[b]
H_2O, pH 7	+0.125 (90)	+0.240 (120)[c]	
EtOH	−0.025 (70)	−0.135 (110)	+0.020 (80)
$PrCO_3$	−0.075 (90)	−0.650[d]	−0.250 (120)
DMF	−0.085 (70)	−0.735 (90)	−0.255 (70)
CH_2Cl_2	−0.100 (60)	[e]	[e]
MeCN	−0.110 (80)	−0.630 (80)	−0.235 (110)
THF	−0.140 (80)	[e]	[e]

[a] Versus SCE. [b] ΔE_p values in parentheses. [c] One wave observed. [d] E_{pa} value; reduction irreversible. [e] Insoluble.

Table VI. Low-Potential Ni(III)/Ni(II) Couples

couple	solvent	$E_{1/2}$,[a] V	ref
$[Ni(emb)]^{1-/2-}$ (**11**)	DMF	−0.035	15
$[Ni(pdtc)_2]^{1-/2-}$ (**3**, **4**)	DMF	−0.085	*b*
	H_2O, pH 7	+0.125	
$[Ni(L)]^{1+/0}$ (**12**)	MeCN	−0.20	14
	H_2O, pH ≥ 8.5	+0.15	
$[Ni(S_2CNEt_2)_3]^{1-/0}$	MeCN	−0.32[c]	57a
$[Ni(dapo)_2]^{1-/2-}$ (**5**, **6**)	DMF	−0.735	*b*
	H_2O, pH 10	+0.055	
$[Ni(nbdt)_2]^{1-/2-}$ (**13**)	DMF	−0.76	16

[a] Versus SCE. [b] This work. [c] Converted to SCE from a different reference electrode.

Of the two presumed d–d bands at 1270 and 782 nm (Figure 1), that at lower energy (7870 cm^{-1}) can now be assigned as $^2A_{1g} \rightarrow {}^2B_{1g}$ in idealized D_{4h} symmetry. The parent state is octahedral ^2E_g, whose degeneracy can be removed by ligand field symmetry or the Jahn–Teller effect. The splitting of these states in the present case is slightly larger than for $[Ni(tacn)_2]^{3+}$[41b] and $[NiF_6]^{3-}$[52] (6500 cm^{-1}) and somewhat less than that in Ni(III) dioximate complexes[24] (9300–10000 cm^{-1}).

(b) $[Ni(dapo)_2]^{1-}$. Because we were unable to isolate this compound, structural information is lacking. The EPR spectrum of an electrochemically generated sample, shown in Figure 6, consists of a broad, nearly isotropic signal with poorly resolved hyperfine splitting of ca. 25 G on the high-field side. The average g value of 2.086 is considered adequate to establish the Ni(III) formulation and the metal-centered nature of the redox couples 2. Other Ni(III) oximate complexes display axial or rhombic spectra with average g values of 2.07–2.10.[14,23,24,53]

Redox Potentials. The solvent dependencies of the redox potentials of reactions 1 and 2 are conveyed by the data in Table V. As would be expected, the potentials are highest in water, which is the most effective solvent for stabilizing the reduced form of a couple, and decrease in aprotic media. The solvent dependence of the $[Ni(pdtc)_2]^{1-/2-}$ couple spans 0.28 V, whereas that for $[Ni(dapo)_2]^{1-/2-}$ is much larger, covering some 0.79 V. This is because of differential solvent interactions with the highly polar oximate group (=N—O⁻), an effect also seen in the solvent dependence of the absorption spectrum of $[Ni(dapo)_2]^{2-}$.[22] On the basis of the acidities of coordinated oximes,[14,54] the dapo complexes are fully deprotonated at pH > 8. Protonation of oximate complexes increases their potentials.[14]

Nickel complexes that are likely to be the most relevant to nickel sites in hydrogenases are those with relatively low $Ni^{III/II}$ redox potentials. Nearly all complexes with potentials below 0 V in aprotic solvents are listed in Table VI.[55] All ligands have the

(48) Pappenhagen, T. L.; Margerum, D. W. *J. Am. Chem. Soc.* **1985**, *107*, 4576.

(49) Accurate anisotropic splitting parameters are expected to be obtained from a single-crystal EPR study of $[^{61}Ni(pdtc)_2]^{1-}$ doped in $(Ph_3PCH_2Ph)[Co(pdtc)_2]$.

(50) Monothiooxalate complexes: (a) Gainsford, G. J.; Jackson, W. G.; Sargeson, A. M. *Aust. J. Chem.* **1980**, *33*, 707. (b) Lydon, J. D.; Mulligan, K. J.; Elder, R. C.; Deutsch, E. *Inorg. Chem.* **1980**, *19*, 2083.

(51) Pyridyl complexes: (a) Szalda, D. J.; Keene, F. R. *Inorg. Chem.* **1986**, *25*, 2795. (b) Bombieri, G.; Polo, A.; Benetollo, F.; Tobe, M.; Humanes, M.; Chatterjee, C. *Acta Crystallogr.* **1987**, *C43*, 1866. (c) Bang, E. *Acta Chem. Scand.* **1977**, *A31*, 495.

(52) Reinen, D.; Friebel, C.; Propach, V. *Z. Anorg. Allg. Chem.* **1974**, *408*, 187.

(53) McAuley, A.; Preston, K. F. *Inorg. Chem.* **1983**, *22*, 2111.

(54) Hanania, G. I. H.; Irvine, D. H.; Shurayh, F. *J. Chem. Soc.* **1965**, 1149.

feature of containing (at least two) anionic sulfur atoms, amidate groups, or oximate groups, alone or in combination. It is these electron-rich, polarizable functionalities that are primarily responsible for the relative stabilization of the Ni(III) state, and, with dithiocarbamates and oximates (including **12**[14]), of the

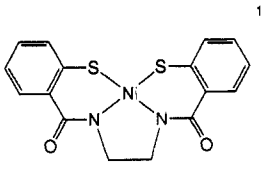

11

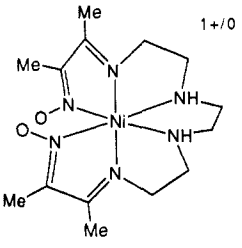

12

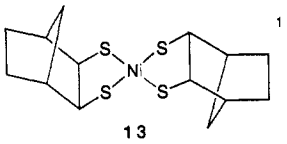

13

Ni(IV) state as well. The first demonstration in classical complexes that anionic sulfur ligands could afford low potentials was made with several $[Ni(S_2CNR_2)_3]^{0/1-}$ couples in 1975.[57] The Ni(III) species are, however, unstable and only one has been isolated.[58] The stabilization of high oxidation states by oximates was recognized much earlier.[12,14] Despite the considerable progress in obtaining low-potential complexes, none of those in Table VI that could be examined in aqueous solution have potentials in the hydrogenase range (ca. −390 to −640 mV). The potentials of the last two couples in DMF are the lowest yet recorded for $Ni^{III/II}$. The large difference in potentials of $[Ni(nbdt)_2]^{1-/2-}$ (**13**) and $[Ni(pdtc)_2]^{1-/2-}$, both of which have a planar NiS_4 group, arises mainly from the effects of less basic sulfur atoms in the latter.[59]

Nickel Sites in Hydrogenase. As noted at the outset, current X-ray absorption spectroscopic results disfavor tetrahedral and planar coordination, are suggestive of a six-coordinate arrangement, and do not disallow five-coordination, for oxidized and fully reduced hydrogenases. $[Ni(pdtc)_2]^{1-}$ possesses the same ground $(d_{z^2})^1$ configuration suggested by the EPR data for certain oxidized hydrogenases, including that from *D. gigas*,[61] although enzyme spectra are generally rhombic (Ni A) rather than axial. Enzyme enrichment with ^{61}Ni leads to splitting of the $g_{\parallel}$ signal with $a_{\parallel}^{Ni}$ values of 26–27 G and $\langle a^{Ni} \rangle \approx 16$ G.[62] The Ni–S distances in this complex are at the upper end of the currently admissible 2.12–2.28-Å range for oxidized *D. gigas* hydrogenase. No ^{14}N hyperfine splittings have been observed for any case in which the foregoing configuration is likely, indicating the absence of axial nitrogen ligands in the Ni A sites. Up to three sulfur ligands are compatible with the EXAFS results for oxidized enzymes.[7,8]

In the fully reduced enzymes, current EXAFS data permit two to four S/Cl atoms at ca. 2.23 Å.[63] Given the Ni–S mean distance of 2.42 Å in $[Ni(pdtc)_2]^{2-}$ and the range 2.4–2.6 Å in other synthetic paramagnetic Ni(II) complexes of thiolates and thioethers, a paramagnetic six-coordinate site appears to be excluded. Further, from MCD spectra,[10] the nickel sites in two reduced enzymes are diamagnetic.

Clearly, more data are required before any firm conclusions about Ni site structures can be drawn. In particular, more and better Ni X-ray absorption data on a larger set of enzymes and synthetic compounds can be anticipated. For now, we suggest the minimal representations five-coordinate **14**[64] for the Ni A site

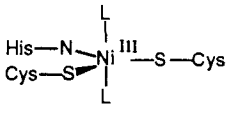

14

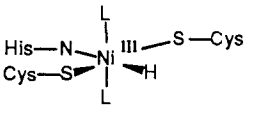

15

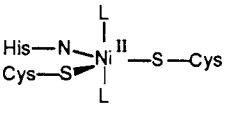

16

(catalytically inactive), six-coordinate **15** for the Ni C site (the first detectable paramagnetic species after reaction with dihydrogen), and five-coordinate **16** for the fully reduced site (a possible resting state in the catalytic cycle). Species L are unidentified but presumably nonnitrogenous ligands.

Summary. The following are the principal results and conclusions of this investigation.

(1) The readily prepared complexes $[Ni(pdtc)_2]^{2-}$ and $[Ni(pdtc)_2]^{1-}$ contain tridentate ligands that adopt a meridional configuration such that each species has an essentially planar NiS_4 group and two trans pyridyl nitrogen atoms. Diamagnetic $[Co(pdtc)_2]^{1-}$ has an analogous structure. The closely related structure of $[Ni(dapo)_2]$ may be assumed to apply, with dimensional changes, to $[Ni(dapo)_2]^{1-}$ and $[Ni(dapo)_2]^{2-}$.

(2) The EPR properties of $[Ni(pdtc)_2]^{1-}$, including ^{61}Ni hyperfine splitting, and its comparative structural features with $[Ni(pdtc)_2]^{2-}$ and $[Co(pdtc)_2]^{1-}$ establish that it is an authentic Ni(III) complex with a ... $(d_{z^2})^1$ ground-state electronic configuration. Similarly, the g_{av} value of $[Ni(dapo)_2]^{1-}$ supports the Ni(III) formulation but the ground-state configuration has not been established.

(3) From (2), redox couples 1 and 2 are metal-centered processes, and $[Ni(pdtc)_2]^{1-}$ has the same ground-state configuration as the Ni(III) sites in oxidized hydrogenases.

(4) Electron-rich, polarizable atoms or groups are the most important intrinsic ligand *electronic* property in the stabilization of Ni(III) and the production of relatively low values of the $Ni^{III/II}$ potential. Such groups include anionic sulfur (of which thiolate is most effective), amidate, and oximate. The value $E_{1/2} = -0.735$ V for $[Ni(dapo)_2]^{1-/2-}$ is one of two lowest known values for a $Ni^{III/II}$ couple. Potentials may also be influenced by ligand *structural* properties that preferentially stabilize one oxidation state on the basis of the size and preferred coordination number of the metal. Such structural influences appear to be small compared to electronic effects in redox couple 1 and, presumably, couple 2.

(5) $[Ni(pdtc)_2]^{2-}$ and $[Ni(pdtc)_2]^{1-}$ are the first pair of structurally defined Ni(II,III) complexes with anionic sulfur ligands. Their EPR and structural properties do not support the proposition (made for alkylthiolate ligation) that the Ni(III) state

(55) Certain unsaturated tetraaza macrocyclic complexes have potentials of ca. −0.3 V or higher.[13] They are omitted from Table VI because of their nonphysiological ligand structure. Also excluded are $[Ni(S_2C_2R_2)_2]^{1-/2-}$ and related dithiolene couples.[56] While their potentials can be as low as −1 V, they do not appear to be candidates for Ni sites in hydrogenases because of their highly delocalized structures and consequently much small **g**-tensor anisotropy.[47]

(56) McCleverty, J. A. In *Reactions of Molecules at Electrodes*; Hush, N. S., Ed.; Wiley-Interscience: New York, 1971, pp 403–492.

(57) (a) Lachenal, D. *Inorg. Nucl. Chem. Lett.* **1975**, *11*, 101. (b) Hendrickson, A. R.; Martin, R. L.; Rohde, N. M. *Inorg. Chem.* **1975**, *14*, 2980.

(58) Willemse, J.; Reuwette, P. H. F. M.; Cras, J. A. *Inorg. Nucl. Chem. Lett.* **1972**, *8*, 389.

(59) As one measure of this effect, the differences in pK_a's for the pairs EtSH/MeCOSH and PhSH/PhCOSH are 7.2 and 4.0, respectively.[60] Further, potentials (E_{pa}, V) for the irreversible oxidations to disulfides in DMF fall in the order $PhCOS^-$ (+0.33), PhS^- (−0.20), EtS^- (−0.49).[17]

(60) (a) Janssen, M. J. In *The Chemistry of Carboxylic Acids and Esters*; Patai, S., Ed.; Interscience, New York, 1969; Chapter 15. (b) Danehy, J. P.; Parameswaran, K. N. *J. Chem. Eng. Data* **1968**, *13*, 386.

(61) Teixeira, M.; Fauque, G.; Moura, I.; Lespinat, P. A.; Berlier, Y.; Prickril, B.; Peck, H. D., Jr.; Xavier, A. V.; LeGall, J.; Moura, J. J. G. *Eur. J. Biochem.* **1987**, *167*, 47.

(62) (a) *D. gigas* hydrogenase: Moura, J. J. G.; Moura, I.; Huynh, B. H.; Krüger, H.-J.; Teixeira, M.; DuVarney, R. C.; DerVartanian, D. V.; Xavier, A. V.; Peck, H. D., Jr.; LeGall, J. *Biochem. Biophys. Res. Commun.* **1982**, *108*, 1388. (b) *M. thermautotrophicum* hydrogenase: Albracht, S. P. J.; Graf, E.-G.; Thauer, R. K. *FEBS Lett.* **1982**, *140*, 311; Kojima, N.; Fox, J. A.; Hausinger, R. P.; Daniels, L.; Orme-Johnson, W. H.; Walsh, C. *Proc. Natl. Acad. Sci. U.S.A.* **1983**, *80*, 378.

(63) Scott, R. A., private communication.

(64) For an example of a distorted trigonal-bipyramidal Ni(III) complex with a ... $(d_{z^2})^1$ ground-state configuration, cf.: Grove, D. M.; van Koten, F.; Zoet, R. *J. Am. Chem. Soc.* **1983**, *105*, 1379.

is actually Ni(II) with a $d_{x^2-y^2}$ electron antiferromagnetically coupled to a ligand thiyl radical.[18] In this event, major changes in Ni–S distances (0.14 Å, Table IV) would not occur, especially when the radical center is likely to be delocalized over most or all sulfur atoms.

In ongoing work, we are examining further combinations of thiolate, amidate, and oximate ligands in chelate ring structures of different sizes as means of modulating the stability of Ni(III) and obtaining systems with hydrogenase reactivity.

Acknowledgment. This research was supported by NSF Grants CHE 85-21365 and CHE 89-03283. X-ray diffraction equipment was obtained by NIH Grant 1 S10 RR 02247. We thank Prof. R. A. Scott for communication of unpublished results.

Supplementary Material Available: Crystallographic data for and details of data collections, thermal and positional parameters, interatomic distances and angles, and calculated hydrogen atom positional parameters for $(Et_4N)_2[Ni(pdtc)_2]$, $(Ph_3PCH_2Ph)[Ni(pdtc)_2]$, and $(Ph_3PCH_2Ph)[Co(pdtc)_2]$ (24 pages); calculated and observed structure factors (79 pages). Ordering information is given on any current masthead page.

Formation and Structure of Alkyl Peroxide Complexes of Germanium(IV) Porphyrins from Direct Reactions with Alkyl Hydroperoxides and by Photolysis of Alkylgermanium(IV) Porphyrins in the Presence of Dioxygen

Alan L. Balch,* Charles R. Cornman, and Marilyn M. Olmstead

Contribution from the Department of Chemistry, University of California, Davis, California 95616. *Received July 13, 1989*

Abstract: $TPPGe(OOCH_2CH_3)_2$ (TPP is the dianion of tetraphenylporphyrin) which has remarkable thermal stability but is hydrolytically sensitive has been prepared by both reaction of ethyl hydroperoxide with $TPPGe(OH)_2$ and by photolysis of $TPPGe(CH_2CH_3)_2$ in the presence of dioxygen. The latter reaction involves successive reactions of the two ethyl groups to give $TPPGe(OOCH_2CH_3)(CH_2CH_3)$ and $TPPGe(OOCH_2CH_3)_2$ and the decomposition/hydrolysis products TPPGe(OH)(CH_2CH_3) and TPPGe(OH)$(OOCH_2CH_3)$. X-ray diffraction studies on both $TPPGe(OOCH_2CH_3)_2$ and $TPPGe(OCH_2CH_3)_2$ confirm their similar, six-coordinate structures. The ring current shifted ^1H NMR resonances of the axial ligands in these complexes are more effective than electronic spectra in monitoring reaction products. Photolysis of $TPPGe(OOCH_2CH_3)_2$ in toluene produces acetaldehyde and ethanol in ratios that are highly temperature dependent. At 23 °C the acetaldehyde/ethanol ratio is 0.55, while at −70 °C it is 3.5.

Recently we have shown that dioxygen reacts with paramagnetic ($S = 1/2$) $PFe^{III}CH_2CH_3$ (P is a tetrarylporphyrin dianion) at −80 °C in toluene solution to form a high spin ($S = 5/2$) alkylperoxo complex (eq 1).[1-4] This intermediate has very little stability and subsequently decomposes even at −80 °C into acetaldehyde and the hydroxy complex $PFe^{III}OH$ (eq 2). Depending on the size of the substituents on the meso phenyl groups of the porphyrin, $PFe^{III}OH$ may then undergo dehydration to form $PFe^{III}OFe^{III}P$ (eq 3).

$$PFe^{III}CH_2CH_3 + O_2 \rightarrow PFe^{III}OOCH_2CH_3 \quad (1)$$

$$PFe^{III}OOCH_2CH_3 \rightarrow PFe^{III}OH + O{=}CHCH_3 \quad (2)$$

$$2PFe^{III}OH \rightarrow PFe^{III}OFe^{III}P + H_2O \quad (3)$$

In toluene $TMPFe^{III}OH$ (TMP is the dianion of tetramesitylporphyrin) catalyzes the decomposition of ethyl hydroperoxide with the formation of acetaldehyde and smaller amounts of ethanol.[3] The formation of acetaldehyde presumably occurs through the two-step mechanism given in eqs 4 and 5. While it has been

$$CH_2CH_3OOH + TMPFe^{III}OH \rightarrow TMPFe^{III}OOCH_2CH_3 + H_2O \quad (4)$$

$$TMPFe^{III}OOCH_2CH_3 \rightarrow TMPFe^{III}OH + O{=}CHCH_3 \quad (5)$$

possible to detect the paramagnetic, five-coordinate intermediate $PFe^{III}OOR$ in these studies, this species is clearly too reactive to allow for its isolation and detailed structural characterization.

In view of the significance of this work to diverse fields including dioxygen activation,[5] enzymatic hydroperoxide decomposition,[6] the synthetic utility of Fe–C bonds,[7] and the behavior of iron-containing oxygenases,[8] we have undertaken to establish the viability of the steps involved in eq 1–5 in a system in which the alkyl peroxide complex is sufficiently stable to isolate. Since it is likely that the decomposition of $PFe^{III}OOCH_2CH_3$ involves cleavage of the O–O bond to form intermediates in higher oxidation states (e.g., $PFe^{IV}{=}O$ or $(P^{\bullet})Fe^{IV}{=}O^+$ where $(P^{\bullet})$ is a porphyrin radical monoanion), it should be possible to obtain and isolate complexes containing an $M–OOCH_2CH_3$ unit by utilizing

(1) Arasasingham, R. D.; Balch, A. L.; Latos-Grazynski, L. *J. Am. Chem. Soc.* **1987**, *109*, 5846.
(2) Arasasingham, R. D.; Balch, A. L.; Latos-Grazynski, L. Studies in Organic Chemistry 33. In *The Role of Oxygen in Chemistry and Biochemistry*; Ando, W.; Moro-Oka, Y.; Eds.; Elsevier: New York, 1988; p 417.
(3) Arasasingham, R. D.; Balch, A. L.; Cornman, C. R.; Latos-Grazynski, L. *J. Am. Chem. Soc.* **1989**, *111*, 4357.
(4) Arasasingham, R. D.; Cornman, C. R.; Balch, A. L. *J. Am. Chem. Soc.* **1989**, *111*, 7800.
(5) *Metal Ion Activation of Dioxygen*; Spiro, T. G., Ed.; Wiley-Interscience: New York, 1980. Sheldon, R. A., Kochi, J. K. *Metal-Catalyzed Oxidations of Organic Compounds*; Academic Press: New York, 1981.
(6) Marnett, L. J.; Weller, P.; Battista, J. R. In *Cytochrome-P450: Structure, Mechanism and Biochemistry*; Ortiz de Montellano, P. R., Ed.; Plenum Press: New York, 1986; p 29.
(7) Corey, E. J.; Nagata, R. *J. Am. Chem. Soc.* **1987**, *109*, 8107. Corey, E. J.; Walker, J. C. *J. Am. Chem. Soc.* **1987**, *109*, 8168.
(8) *Molecular Mechanisms of Oxygen Activation*; Hayaishi, O.; Ed.; Academic Press: New York, 1974. Ortiz de Montellano, P. R. *Cytochrome P-450*; Plenum Press: New York, 1986.

0002-7863/90/1512-2963$02.50/0